Electronic Supplementary Material (ESI) for Environmental Science: Nano.

Supplementary Information

Facet-specific cation exchange and heterogeneous transformation of cadmium sulfide nanoparticles induced by Cu(II)

Meiying Huang[a,b], Cun Liu[a], Peixin Cui[a], Fei Dang[a], Jing Zhou[a], Mengli Liu[a], Yujun Wang[a,b*]

[a] Key Laboratory of Soil Environment and Pollution Remediation, Institute of Soil Science Chinese Academy of Sciences, Nanjing 210008, China

[b] University of Chinese Academy of Sciences, Beijing 100049, China

*Corresponding author, Tel: 0086-25-86881182, E-mail: yjwang@issas.ac.cn

Text S1 Chemicals

$Cd(CH_3COO)_2·2H_2O$ (CAS no.: 5743-04-4), $Cd(NO_3)_2·4H_2O$ (CAS no.: 10022-68-1), $Cu(NO_3)_2·3H_2O$ (CAS no.: 10031-43-3), thiourea (CAS no.: 62-56-6), and acetic acid (AA, CAS no.: 64-19-7) were purchased from Sinopharm Chemical Reagent Co., Ltd (Shanghai, China). $CdCl_2·2.5H_2O$ (CAS no.: 7790-78-5) and malic acid (MA, CAS no.: 97-67-6) were obtained from Shanghai Macklin Biochemical Co., Ltd. Diethylenetriamine (DETA, CAS no.: 111-40-0), 2-(N-Morpholino)ethanesulfonic acid (MES, CAS no.: 4432-31-9) and sulfur (S, CAS no.: 7704-34-9) were obtained from Sigma-Aldrich (Shanghai) Trading Co. Ltd. (China). Ethylenediamine, ethylene diamine tetraacetic acid (EDTA, CAS no.: 60-00-04), citric acid (CA, CAS no.: 77-92-9), oxalic acid (OA, CAS no.: 144-62-7), tartaric acid (TA, CAS no.: 87-69-4), NaOH (CAS no.: 1310-73-2), HNO_3 (CAS no.: 7697-37-2), and $NaNO_3$ (CAS no.: 7631-99-4) were purchased from Nanjing Chemical Reagent Co., Ltd.

Text S2 Preparation of CdS-NPs

i CdS-sphere, CdS-rod, CdS-sheet

Different cadmium salts and sulfur sources were used to synthesize CdS-NPs with different morphologies, that is, three CdS-NPs (CdS-sphere, CdS-rod, and CdS-sheet) and one nanosized biogenic CdS (Bio-CdS NPs).[1]

For the synthesis of CdS-sphere, 3.2 mmol $Cd(CH_3COO)_2·2H_2O$ and 16 mmol thiourea were dissolved in 40 mL deionized water, after being stirred in 25℃ for 30

min, the mixture was transferred into a Teflon-lined stainless steel autoclave with a capacity of 100 mL. The mixture was maintained at 140℃ for 5 h. After that, the autoclave was cooled to room temperature. The final products were centrifuged and washed with ethanol and deionized water, and then dried at 60 °C in a vacuum oven for 12 h.

$Cd(NO_3)_2·4H_2O$ and ethylenediamine were used to synthesize CdS-rod. 2 mmol $Cd(NO_3)_2·4H_2O$ was added into 60 mL ethylenediamine. After being stirred for 10 min, 16 mmol thiourea was added. The mixture was transferred into a Teflon-lined stainless steel autoclave with a capacity of 100 mL after being stirred for 10 min, the autoclave was heated at 170℃ for 12 h. The final products were centrifuged and washed with ethanol and deionized water, and then dried at 60 °C in a vacuum oven for 12 h.

$CdCl_2·2.5H_2O$ and S powder were used to synthesize CdS-sheet. 0.336 g $CdCl_2·2.5H_2O$ and 0.320 g S powder were added to 60 mL DETA. The mixture was vigorously stirred for 30 min to form a homogeneous suspension and then was transferred into a Teflon-lined stainless steel autoclave with a capacity of 100 mL. The autoclave was heated at 80℃ for 48 h. After that, the autoclave was cooled to room temperature. The final products were centrifuged and washed with ethanol and deionized water, and then dried at 60 °C in a vacuum oven for 12 h.

ii CdS-rod6, CdS-rod12, CdS-rod24

For the preparation of CdS-rod NPs, 6.224 mmol $Cd(NO_3)_2·4H_2O$ was added to 60 mL ethylenediamine. After being stirred for 10 min, 18.655 mmol thiourea was

added. The mixture was transferred into a Teflon-lined stainless steel autoclave with a capacity of 100 mL after being stirred for another 10 min, the autoclave was heated at 180℃ for 6, 12, or 24 h, and the corresponding products were named CdS-rod6, CdS-rod12, and CdS-rod24, respectively. After that, the autoclave was cooled to room temperature. The final products were centrifuged and washed with deionized water, and then dried at 60 °C in a vacuum oven for 12 h.[2]

iii Bio-CdS NPs

Sulfate-reducing bacteria (SRB), which was obtained from paddy soil, was used to synthesize Bio-CdS NPs. The boiled culture medium (40 mL) was placed in a 100 mL serum bottle, the top space of bottle was purified with N_2, and then the serum bottle was sealed and sterilized at 120℃ for 20 min.[3] Paddy soil (2 g) was added to the above culture medium in a glovebox purged with N_2. The fifth generation of bacterial suspension, which was enriched with SRB, was used to synthesize Bio-CdS NPs. The $CdCl_2$ solution (100 mM) was taken into the culture medium. After 3 weeks of incubation (30℃), the bacterial suspension was taken out in the glove box, and then centrifuged at 12987 g for 15 min. The precipitate was washed more than 4 times with oxygen-free water and then freeze-dried.[1]

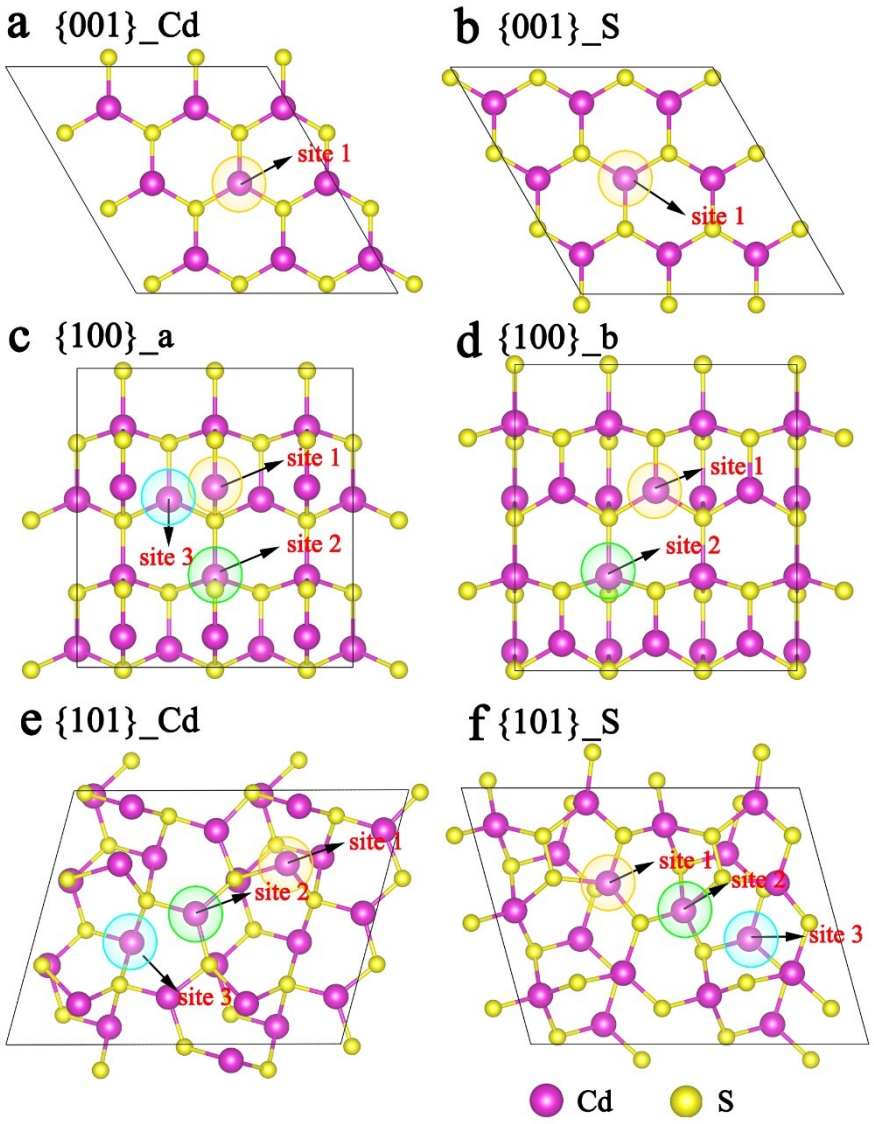

Fig. S1 The Cd/Cu exchange sites in CdS slab models with different facets (top view).

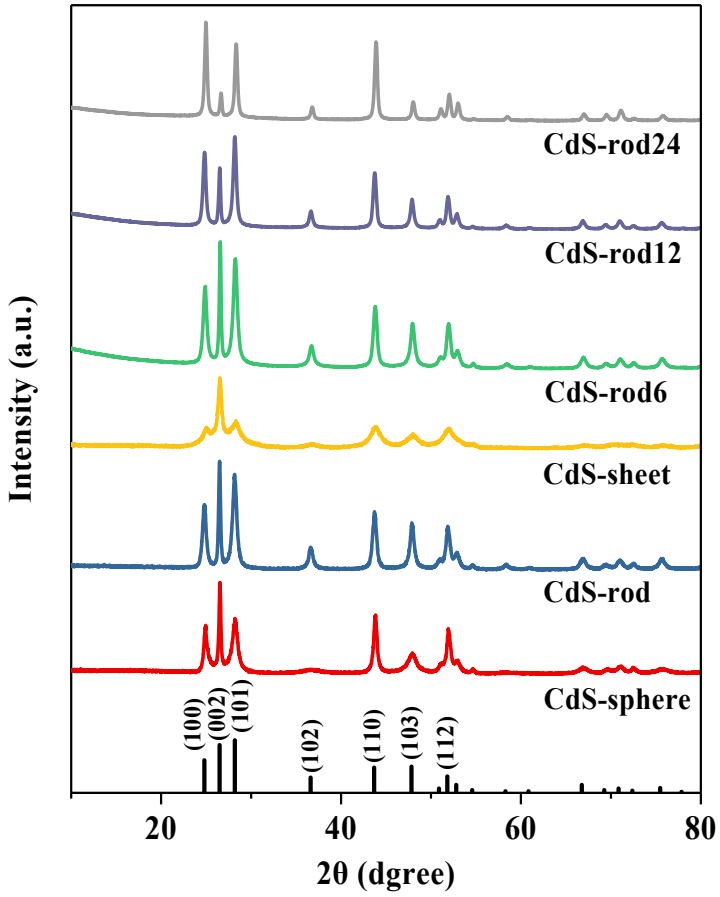

Fig. S2 XRD patterns of CdS-NPs, in which the XRD patterns of CdS-sphere, CdS-rod, CdS-sheet from ref 1.

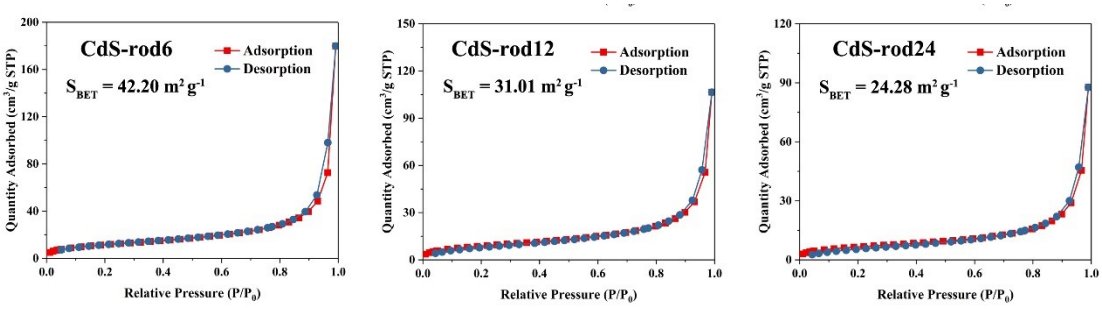

Fig. S3 N_2 adsorption-desorption isotherms and SSA (S_{BET}) of CdS-rods.

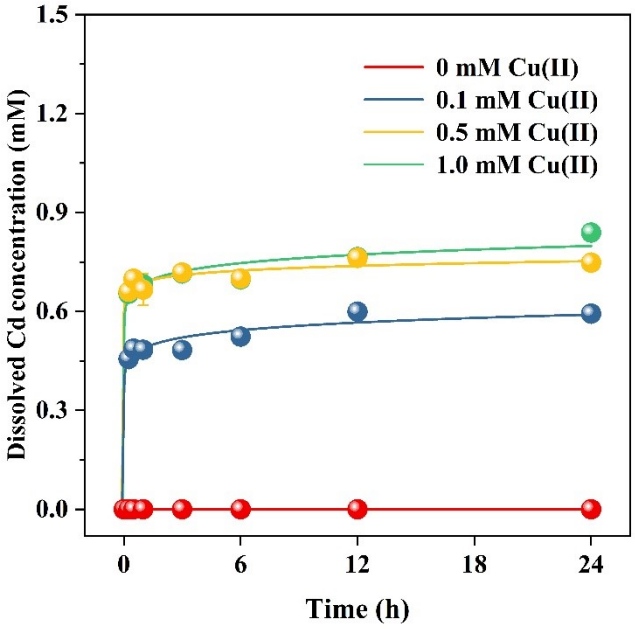

Fig. S4 Dissolution kinetics of Bio-CdS NPs in presence of Cu(II).

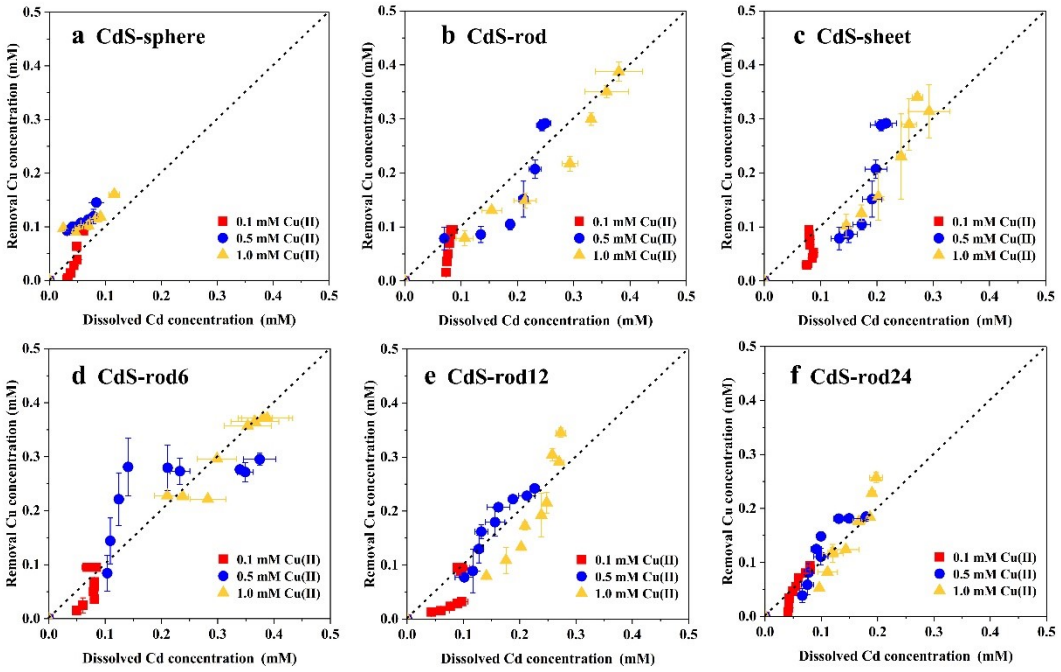

Fig. S5 The ratio of dissolved Cd(II) to removed Cu(II) in the CdS-NP suspensions during the reaction process of CdS-NPs with Cu(II).

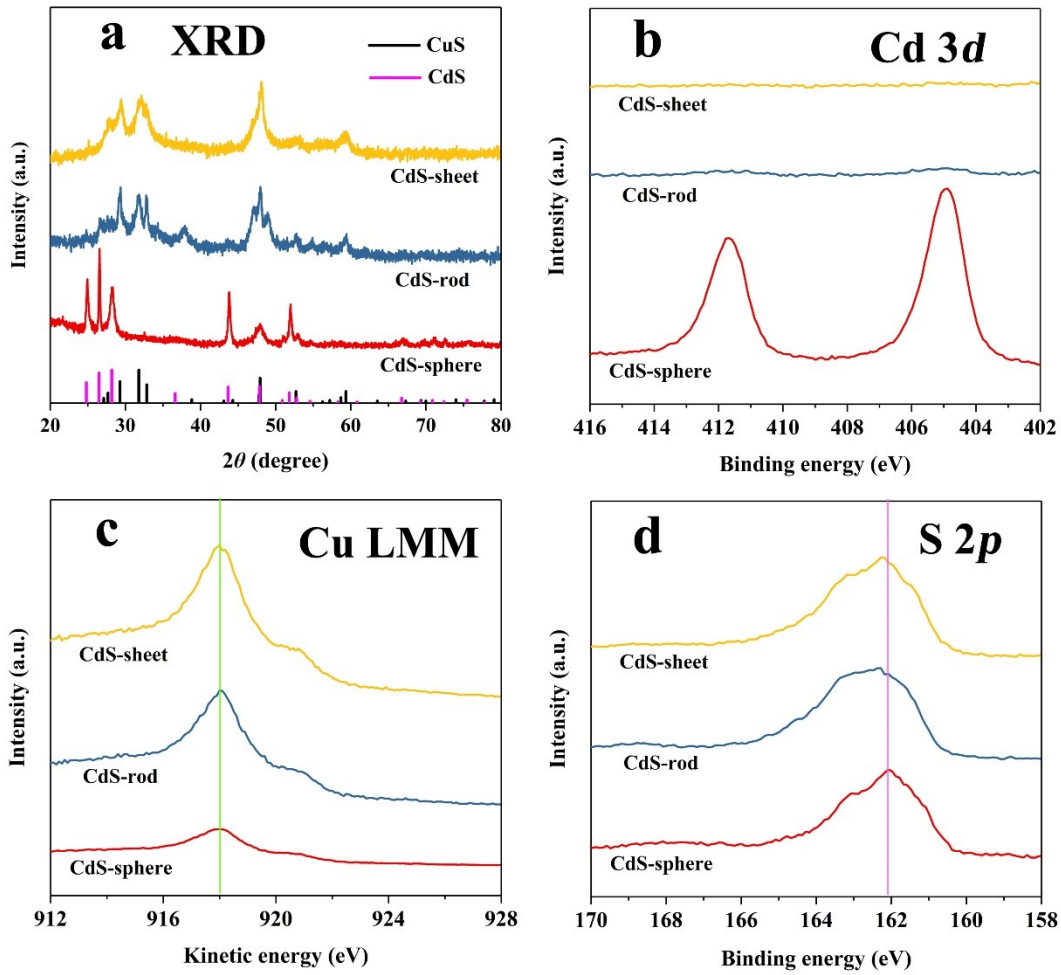

Fig. S6 XRD patterns (a), Cd 3*d* (b), S 2*p* (d) XPS spectra, and X-ray-excited Cu (LMM) AES spectra (c) of the precipitates upon the interaction with CdS-NPs and 10 mM Cu(II) for 24 h.

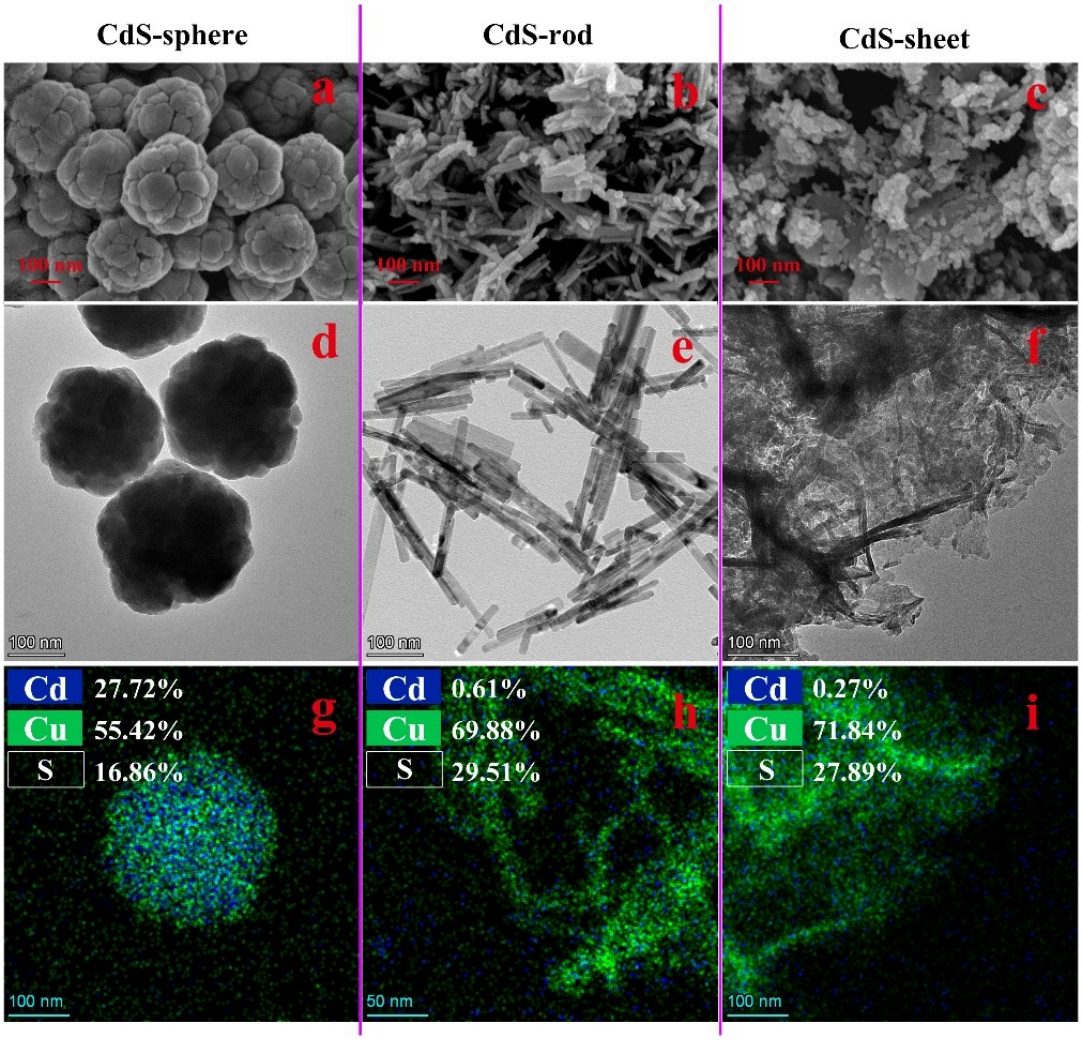

Fig. S7 SEM (a–c), TEM (d–f), and elemental mapping (g–f) images of the precipitates upon the interaction with CdS-NPs and 10 mM Cu(II) for 24 h. Cd, Cu, and S mass fraction (%) are present in elemental mapping images.

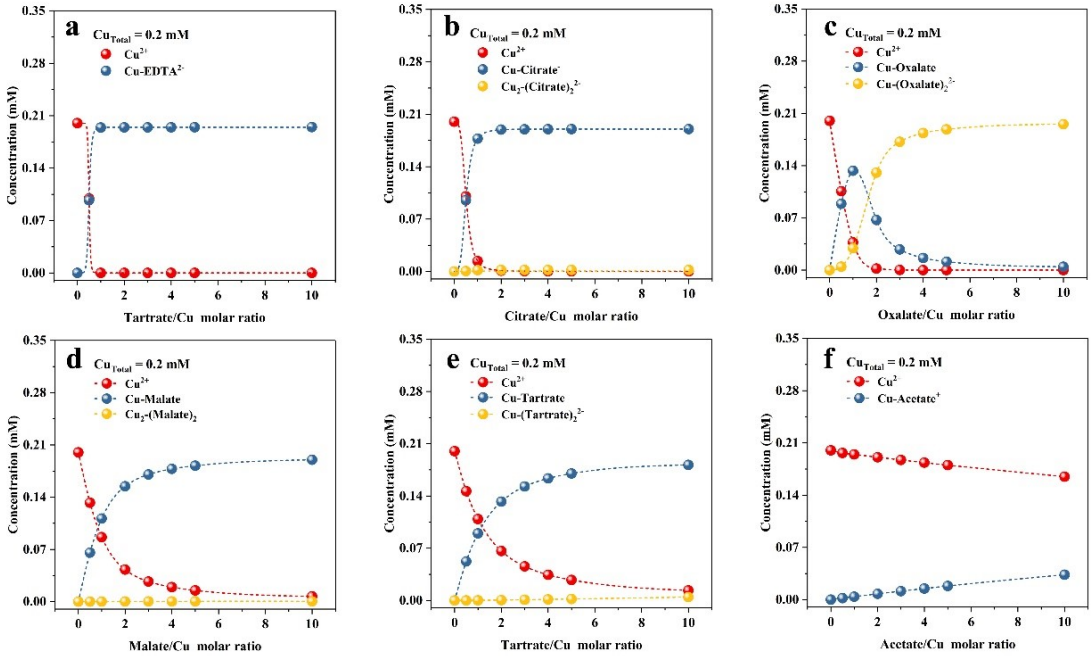

Fig. S8 The chemical speciation distribution of Cu simulated by MINTEQ under different mole ratios of LMWCAs and total Cu (pH = 5.0).

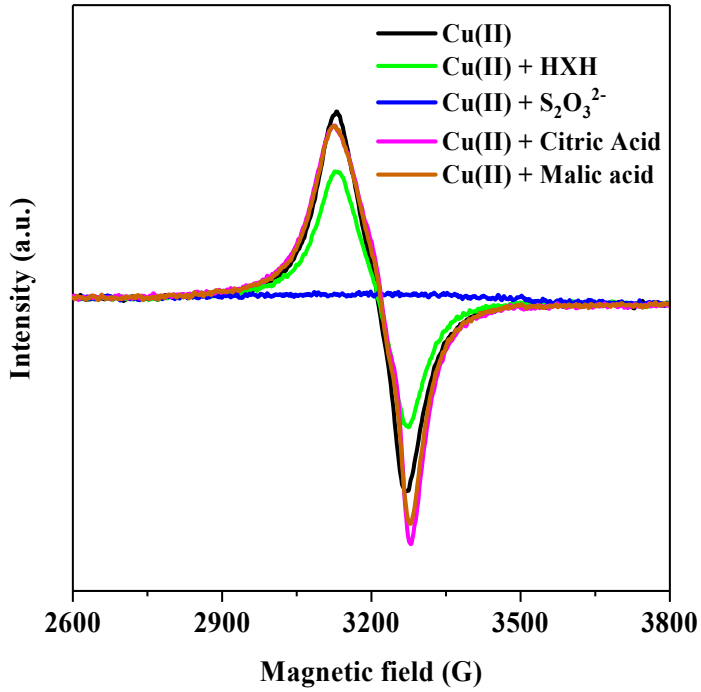

Fig. S9 EPR spectra of solutions upon the interaction with 10 mM Cu(II) and 50 mM reducing substances for 5 min.

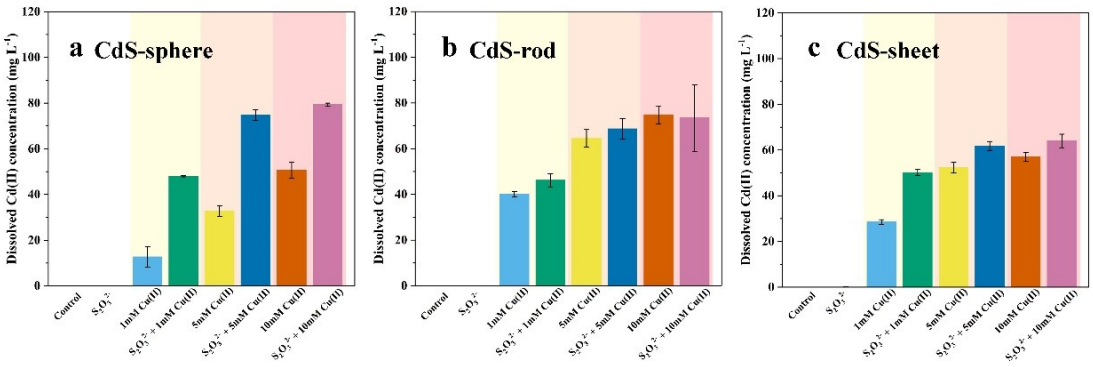

Fig. S10 Dissolved Cd(II) concentrations in CdS-NP suspensions upon the interaction with 10 mM Cu(II) and 50 mM $S_2O_3^{2-}$ for 24 h.

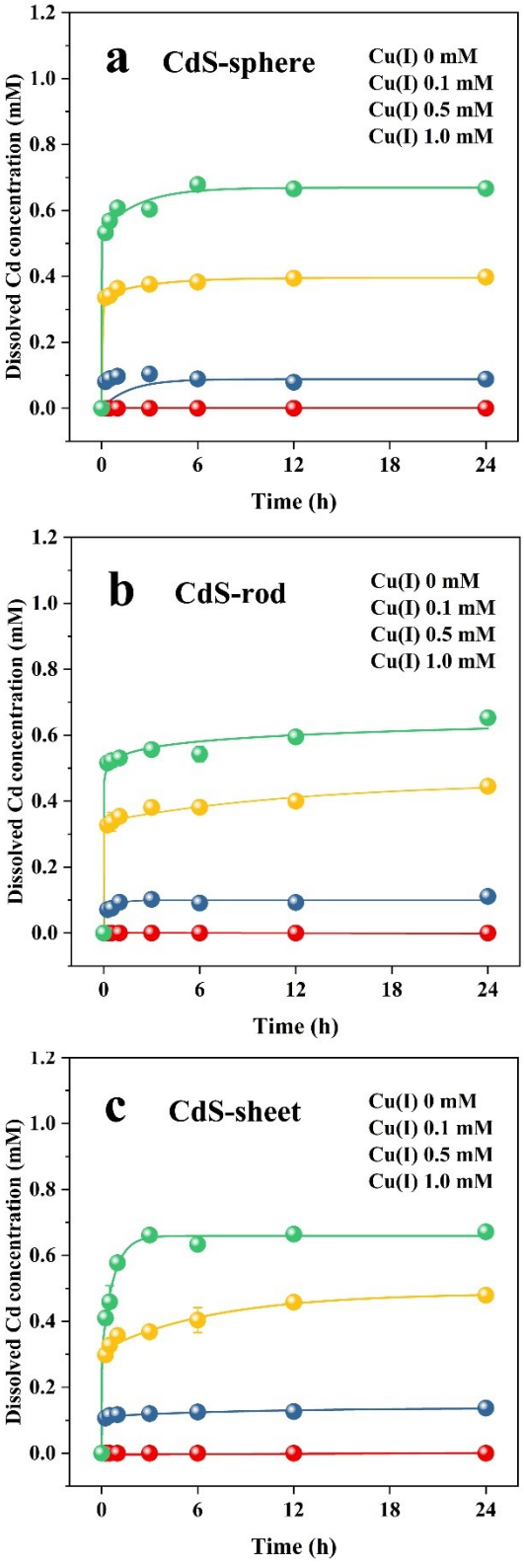

Fig. S11 Dissolution kinetics of CdS-sphere (a), CdS-rod (b), and CdS-sheet (c) in presence of Cu(I).

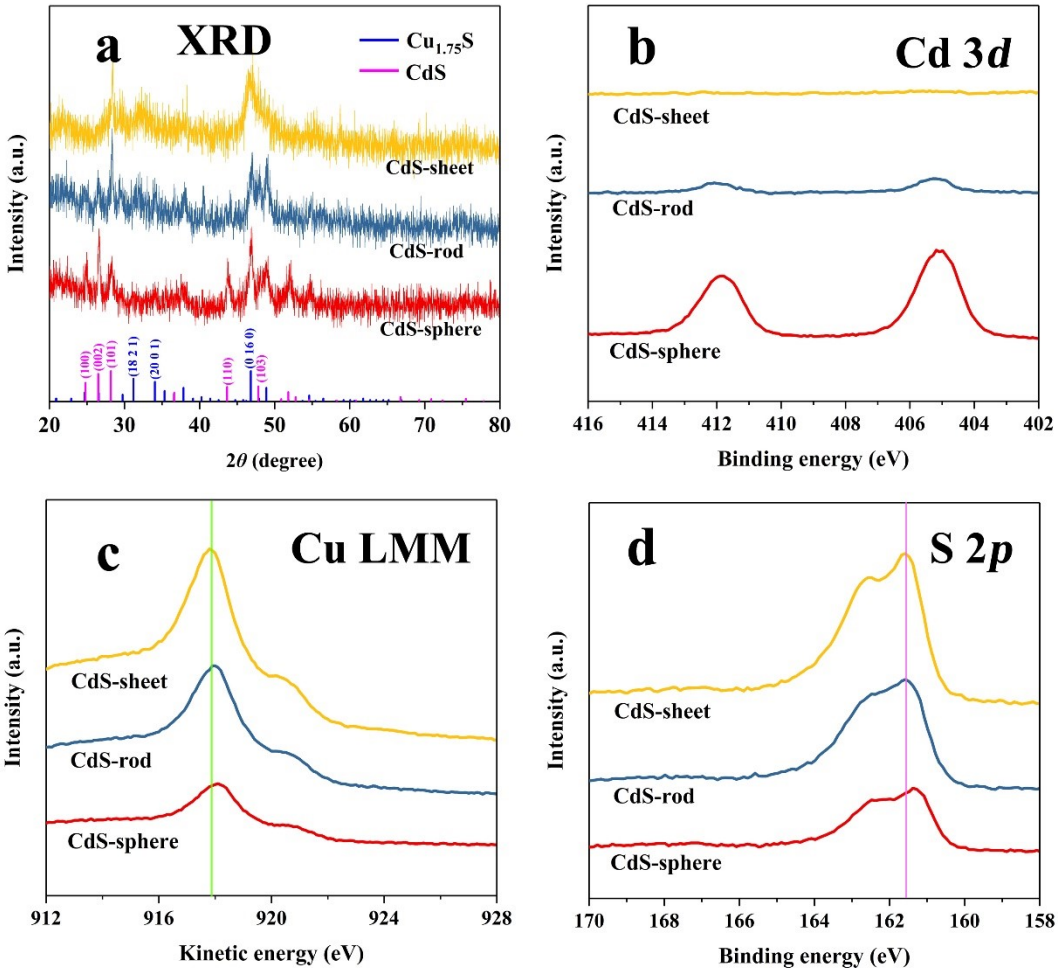

Fig. S12 XRD patterns (a), Cd 3*d* (b), S 2*p* (d) XPS spectra, and X-ray-excited Cu (LMM) AES spectra (c) of the precipitates upon the interaction with CdS-NPs and 1 mM Cu(I) for 24 h.

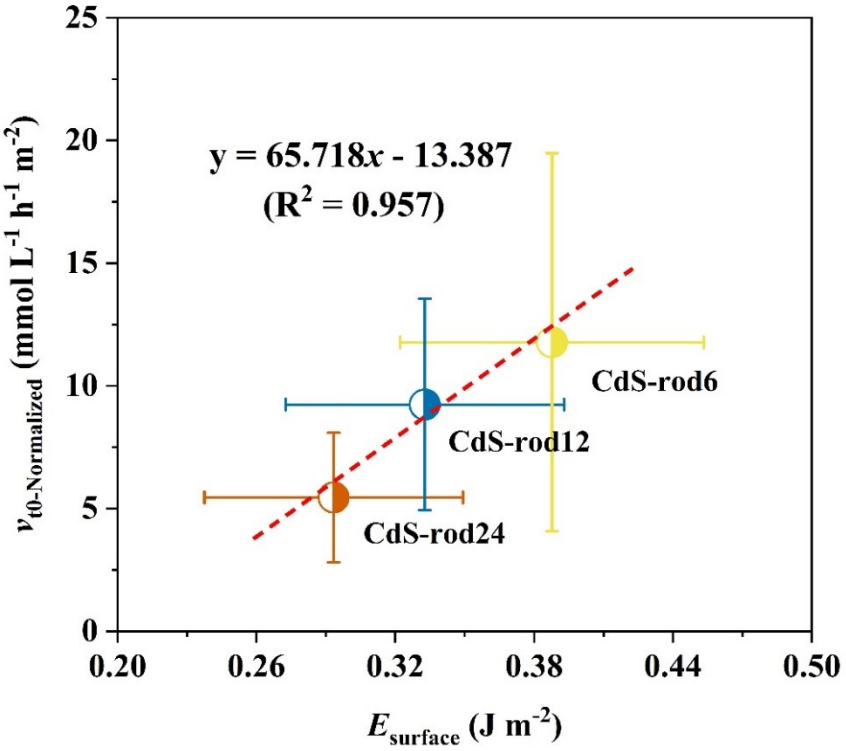

Fig. S13 The relationship between the surface energy ($E_{Surface}$) and the initial dissolution rate normalized by SSA ($v_{t0\text{-}Normalized}$) of CdS-rods.

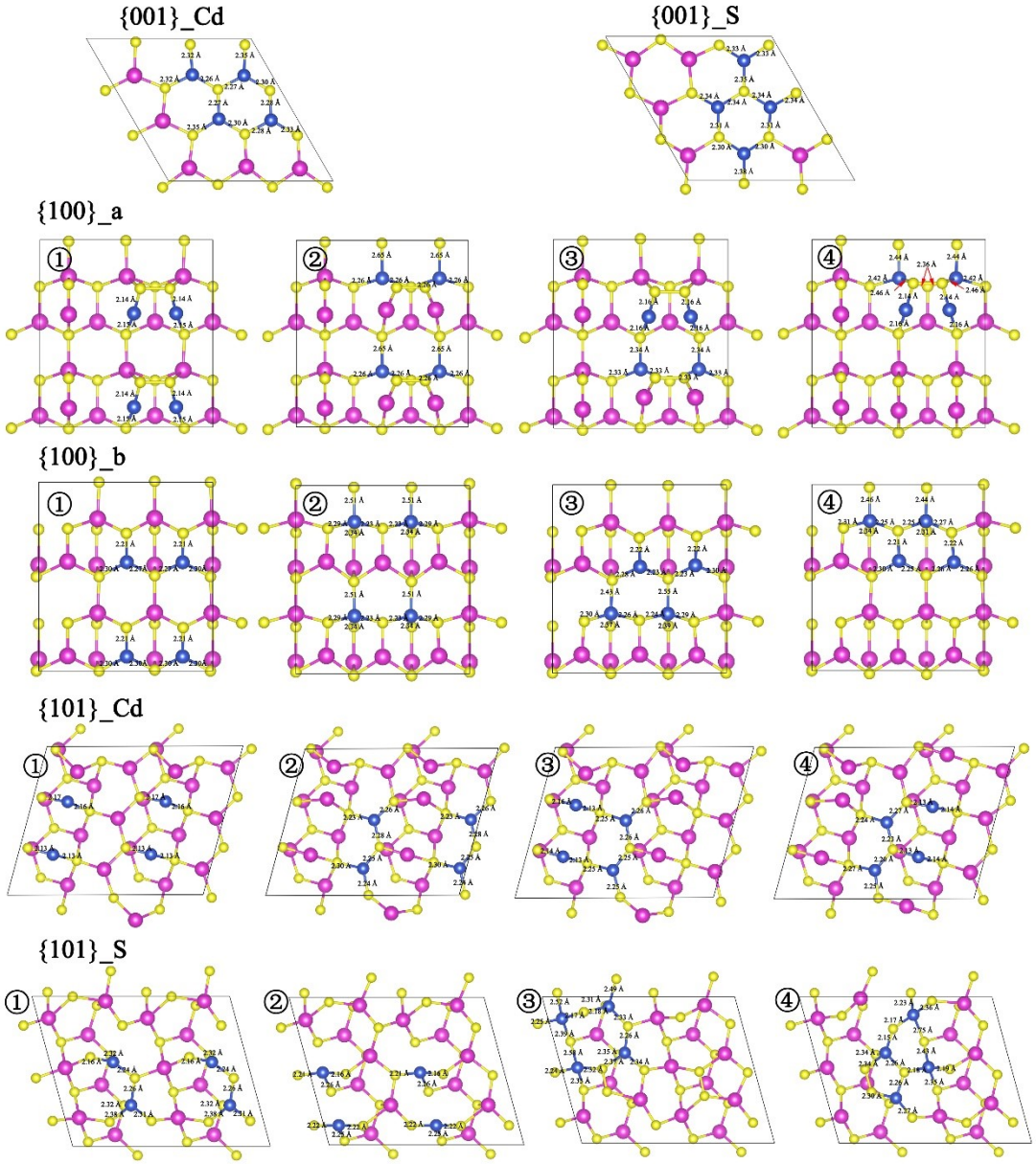

Fig. S14 Optimized structures obtained by DFT calculations after the cation exchange of Cd(II) by Cu(II) on the CdS slab models with different exposed facets. Color scheme: Cd: magenta, S: yellow, Cu: blue.

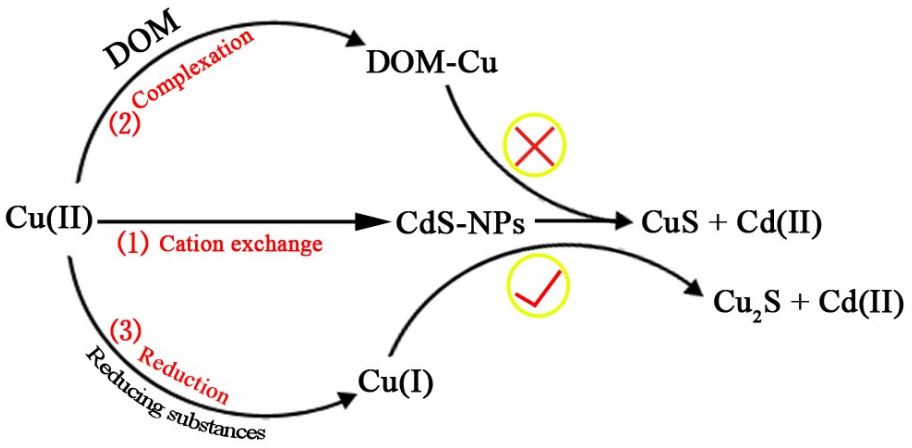

Fig. S15 The effect mechanisms of DOM and reducing substances during the dissolution of CdS-NPs in the presence of Cu(II). (DOM-Cu: the Cu(II) complexed with DOM). Detail information about these reactions was shown as followed text:

(1) $CdS_{(s)} + Cu(II) \rightarrow CuS_{(s)} + Cd(II)$

The dissolution mechanism of CdS-NPs by cation exchange in the presence of dissolved Cu(II) ions.

(2) $Cu(II) + DOM \rightarrow DOM\text{-}Cu$

The complexation of Cu(II) with DOM inhibited the cation exchange on CdS-NPs by Cu(II).

(3) $Cu(II) + \text{reducing substances} \rightarrow Cu(I)$

$CdS_{(s)} + 2Cu(I) \rightarrow Cu_2S_{(s)} + Cd(II)$

The reduction of Cu(II) by reducing substances in an anaerobic environment, and the resulting Cu(I) promoted the dissolution of CdS-NPs by the Cd(II)/Cu(I) cation exchange.

Table S1. The information about the low-molecular-weight carboxylic acids (LMWCAs) used in this study.

Molecular	Molecular weight	CAS number	Molecular structure	pK_a of the carboxyl group	Stability constant for CuL complex logK [a]
Acetic acid	60.05	64-19-7	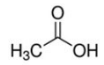	pK_a = 4.76	1.83
Citric acid	192.12	77-92-9	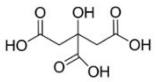	pK_{a1} = 3.13 pK_{a2} = 4.76 pK_{a3} = 6.40	5.90
Malic acid	134.09	97-67-6	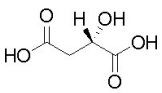	pK_{a1} = 3.40 pK_{a2} = 5.20	3.42
Oxalic acid	90.03	144-62-7	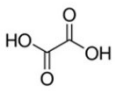	pK_{a1} =1.20 pK_{a2} =4.28	4.84
Tartaric acid	150.09	87-69-4	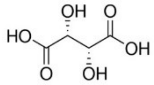	pK_{a1} =2.98 pK_{a2} =4.34	3.39
Ethylene diamine tetraacetic acid	292.24	60-00-4	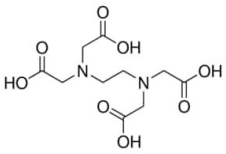	pK_{a1} = 0.00 pK_{a2} = 1.50 pK_{a3} = 2.00 pK_{a4} = 2.66	18.80

[a]. Data from Martell, A.E. and Smith, R.M. 1974 Critical stability constants, Plenum Press, New York.

Table S2. Characterization of soils used to extract soil pore water

Soil	pH[a]	OM[b] (g kg^{-1})	Metal concentration[c] (mg kg^{-1})		(g kg^{-1})	
			Cu	Cd	Fe	Mn
JL	7.9	33.30	21.57	0.23	29.51	0.61
JS	7.3	34.34	22.43	0.29	30.98	0.28
HN	6.4	35.71	23.17	0.42	34.62	0.52
YN	6.9	26.52	29.26	0.39	31.37	0.20
ZJ	6.2	26.83	37.10	0.26	34.01	0.35

[a] Soil pH was determined in carbon dioxide-free Milli-Q water at a soil to solution ratio of 1:2.5 (m/v).

[b] Organic matter concentration was determined using the Walkley-Black (WB) titration method before K_2CrO_4-H_2SO_4 oxidation.

[c] Metal concentrations were determined by ICP-MS or ICP-OES after microwave digestion of the samples.

Table S3. The average dimensions and exposed facets of CdS-NPs

CdS-NPs	Dimension (nm)	Exposed facet (%)	$SSA_{\{Exposed\ facet\}}$ ($m^2\ g^{-1}$)
CdS-sphere*	Diameter = 260	{101} (63%)	4.62
		{100} (36%)	2.64
CdS-rod*	Length = 147 Diameter = 23	{100} (87%)	31.96
		{101} (8%)	2.94
		{001} (5%)	1.94
CdS-sheet*	Lateral size = 280	{001} (95%)	60.07
		{100} (5%)	3.16
CdS-rod6	Length = 125 Diameter = 20	{100} (81%)	34.18
		{101} (5%)	2.11
		{001} (14%)	5.91
CdS-rod12	Length = 285 Diameter = 27	{100} (89%)	27.60
		{101} (3%)	0.93
		{001} (8%)	2.48
CdS-rod24	Length = 681 Diameter = 40	{100} (95%)	23.07
		{101} (1%)	0.24
		{001} (4%)	0.73

* The average dimension, exposed facets, and SSA of CdS-sphere, CdS-rod, and CdS-sheet were quoted from ref 1.

Table S4. The initial dissolution rate (v_{t0}) and initial dissolution rate normalized by the specific surface area ($v_{t0\text{-Normalized}}$) of CdS-NPs in the presence of Cu(II)

	Cu(II) (mM)	v_{t0} (mmol L^{-1} h^{-1})	$v_{t0\text{-Normalized}}$ (mmol L^{-1} h^{-1} m^{-2})
CdS-sphere	0.1	0.038 ± 0.002	2.578 ± 0.140
	0.5	0.042 ± 0.003	2.829 ± 0.179
	1.0	0.056 ± 0.007	3.818 ± 0.459
CdS-rod	0.1	0.077 ± 0.006	5.236 ± 0.424
	0.5	0.187 ± 0.007	12.744 ± 0.504
	1.0	0.214 ± 0.020	14.547 ± 1.365
CdS-sheet	0.1	0.087 ± 0.005	5.945 ± 0.338
	0.5	0.173 ± 0.016	11.791 ± 1.075
	1.0	0.202 ± 0.007	13.789 ± 0.458
CdS-rod6	0.1	0.079 ± 0.001	5.405 ± 0.060
	0.5	0.141 ± 0.006	9.582 ± 0.427
	1.0	0.299 ± 0.032	20.342 ± 2.176
CdS-rod12	0.1	0.077 ± 0.006	5.227 ± 0.420
	0.5	0.128 ± 0.008	8.691 ± 0.559
	1.0	0.203 ± 0.005	13.795 ± 0.319
CdS-rod24	0.1	0.043 ± 0.002	2.914 ± 0.122
	0.5	0.077 ± 0.002	5.261 ± 0.158
	1.0	0.120 ± 0.008	8.181 ± 0.563

Table S5. Characterization of soil pore water

Soil pore water[a, b]	pH	TOC (mg C L^{-1})	Free Cu concentration (mM)
DOM_{JL}	8.3	43.74	/
DOM_{JS}	7.6	41.83	/
DOM_{HN}	6.9	48.45	/
DOM_{YN}	6.7	63.85	/
DOM_{ZJ}	8.0	61.90	/
Cu(II)-DOM_{JL}	8.3	43.74	0.32×10^{-3}
Cu(II)-DOM_{JS}	7.6	41.83	3.04×10^{-3}
Cu(II)-DOM_{HN}	6.9	48.45	124.70×10^{-3}
Cu(II)-DOM_{YN}	6.7	63.85	28.86×10^{-3}
Cu(II)-DOM_{ZJ}	8.0	61.90	9.36×10^{-3}

[a] Soil pore water were extracted at a soil to solution ratio of 1:2 (m/v). The soil suspension was centrifuged (10000 rpm) after shaking (200 rpm) for 12 h, and then the supernatant were filtered by 0.45 μm filter membranes.

[b] Cu(II) spiked soil pore water were obtained by adding $Cu(NO_3)_2$ stock solution to the soil pore water, and total Cu concentration in Cu(II) spiked soil pore water was 0.2 mM.

References

1. M. Huang, C. Liu, P. Cui, T. Wu, X. Feng, H. Huang, J. Zhou and Y. Wang, Facet-dependent photoinduced transformation of cadmium sulfide (CdS) Nanoparticles, *Environ. Sci. Technol.*, 2021, **55**, 13132-13141.
2. F. Vaquero, J. L. G. Fierro and R. M. N. Yerga, From Nanorods to Nanowires of CdS Synthesized by a Solvothermal Method: Influence of the Morphology on the Photoactivity for Hydrogen Evolution from Water, *Molecules*, 2016, **21**.
3. C. Chen, L. Y. Li, K. Huang, J. Zhang, W. Y. Xie, Y. H. Lu, X. Z. Dong and F. J. Zhao, Sulfate-reducing bacteria and methanogens are involved in arsenic methylation and demethylation in paddy soils, *Isme J.*, 2019, **13**, 2523-2535.